Asian Journal of Chemistry; Vol. 26, No. 19 (2014), 6492-6498

ASIAN JOURNAL OF CHEMISTRY

http://dx.doi.org/10.14233/ajchem.2014.16474

γ-Fe_2O_3@Polyaniline-Chlorambucil Synthesized by Using Doping/Dedoping Method of Polyaniline

QIAN SHEN, JIANPING LANG and JINQING KAN*

School of Chemistry and Chemical Engineering, Yangzhou University, Yangzhou 225002, P.R. China

*Corresponding author: Fax: +86 514 87975590 8410; Tel: +86 514 87975590 9415; E-mail: jqkan@yzu.edu.cn

Received: 5 October 2013; *Accepted*: 19 November 2013; *Published online*: 16 September 2014; AJC-15947

The γ-Fe_2O_3@polyaniline-chlorambucil composite has been synthesized. The γ-Fe_2O_3@PANI is modified by chlorambucil (CHB, a chemotherapeutic drug) based on the unique doping-dedoping mechanism of the polyaniline, which don't change doped groups of the chlorambucil. It is confirmed by XRD, VSM, FT-IR and TEM that the chlorambucil was doped into γ-Fe_2O_3@PANI. The experimental results showed that the γ-Fe_2O_3@PANI-CHB has the superparamagnet, electrochemical activity and good conductivity. The poly(vinyl, pyrrolidone) surfactant could improve the suspensibility of γ-Fe_2O_3@PANI-CHB in the aqueous solution. The γ-Fe_2O_3@PANI-CHB could be concentrated in a magnetic field. The concentration of the γ-Fe_2O_3@PANI-CHB at 3000 Gauss was 6 times higher than that of the original solution at a flow rate of 0.1118 g s^{-1}. The results showed that γ-Fe_2O_3@PANI-CHB can kill Madin Darby Canine Kidney (MDCK) but there is no toxic effect of γ-Fe_2O_3@PANI on Madin Darby Canine Kidney cells.

Keywords: Polyaniline, γ-Fe_2O_3, Chlorambucil, Superparamagnetism, Nano-composite.

INTRODUCTION

Since MacDiarmid *et al.*[1] redeveloped polyaniline in 1984, polyaniline with its good thermal stability, chemical stability and electrochemical reversibility, excellent electromagnetic microwave absorption properties, low price of raw materials, simple synthetic method and unique doping-dedoping mechanism[2-6], has become a research hotspot as the most promising conductive polymer materials[7-10]. In recent years, conductive polyaniline and inorganic material composite[11-16] caused a great deal of interest, because the composite can improve performance of original material. Currently polyaniline composite material applied in many fields, such as all-plastic metal anticorrosion technology, electromagnetic shielding technology, antistatic technology, electrochromic, solar batteries, sensor elements, catalytic materials, stealth technology. Above all, polyaniline has good biological compatibility[17-20]. The conductivity of polyaniline can last about 100 h in human body and currents through the conductor surfaces can control the shape and function of anchorage-dependent cells[21]. So polyaniline can also be used as a carrier material in the magnetic targeting drug delivery system.

The magnetic nanoparticles (such as γ-Fe_2O_3 and Fe_3O_4) has the advantage of chemical stability and biocompatibility and can be excreted out of the body regularly, while magnetic materials such as cobalt and nickel have certain physiological toxicity, the γ-Fe_2O_3 and Fe_3O_4 are usually applied to the biological field[22,23].

Chlorambucil (CHB)[24-29], a kind of nitrogen mustard derivatives, has an inhibition effect on a variety of tumor such as chronic lymphocytic leukemia, lymphosarcoma, ovarian cancer, breast cancer, villous epithelial tumors and multiple myeloma. However, due to the poor specificity, highly toxic and chemical instability, the application of chlorambucil has been extremely limited. If chlorambucil is doped into polyaniline, it can avoid the problem of changing the structure of its pharmacological groups, improve the efficacy and reduce toxicity to the normal tissue by the application of the external magnetic field.

In our study, we mainly focus on the synthesis and characterizations of γ-Fe_2O_3@polyaniline-chlorambucil composite. The γ-Fe_2O_3@PANI not only can reduce the reunion between the particles, but also the polyaniline can provide functional group to load drug. The γ-Fe_2O_3@PANI-CHB is synthesized by the application of unique doping-dedoping mechanism of the polyaniline[30,31], which don't change the structure of doped groups. The study may provide an academic foundation for developing some new drugs of anticancer.

EXPERIMENTAL

All chemicals used were analytical grade. The monomer aniline was distilled under reduced pressure and stored in refrigerator (about 4 °C) before use. Ammonium persulfate (APS), ammonium hydroxide (30 % NH_3 in water), dimethyl formamide (DMF) and other chemicals were used as received

without further treatment. 1-Ethyl-3-methylimidazolium ethyl sulfate (EMIES) ionic liquid was synthesized by the method of Holbrey *et al.*[32]. All of the aqueous solutions were prepared with double distilled water. The Britton-Robinson (BR) buffer solution, being made up of 0.04 M phosphoric acid, 0.04 M acetic acid, 0.04 M boric acid, 0.2 M sodium hydroxide, was used to adjust the acidity of the solution[33]. The Madin Darby Canine Kidney (MDCK) cells were provided by College of Animal Science of Yangzhou University.

Synthesis of γ-Fe_2O_3@PANI-CHB: The γ-Fe_2O_3 and γ-Fe_2O_3@PANI nanoparticles were prepared according to published procedures with some modifications[34,35]. Since chlorambucil is insoluble in water, certain amount of chlorambucil was dissolved in the ethanol and the appropriate amount of γ-Fe_2O_3@PANI aqueous solution was added. The mixed solution was constantly stirred for 12 h, then filtered and washed with the ethanol and double distilled water. The primary products were transferred to the beaker and stirred for 3 h meanwhile adding moderate amounts of hydrochloric acid to improve the conductivity of γ-Fe_2O_3@PANI. The product was filtered, washed with double distilled water and dried for 12 h in 50 °C of vacuum oven. The γ-Fe_2O_3@PANI-CHB was obtained. The schematic for the preparation of γ-Fe_2O_3@PANI-CHB is shown in Fig. 1.

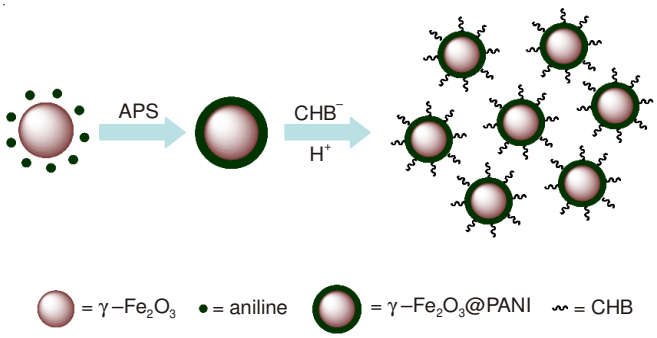

Fig. 1. Schematic illustration of the formation of γ-Fe_2O_3@PANI-CHB

Characterization of γ-Fe_2O_3@PANI-CHB: The γ-Fe_2O_3@PANI, γ-Fe_2O_3@PANI-CHB and chlorambucil were respectively dissolved in the DMF and measured in the range from 250 to 900 nm by UV-visible spectrophotometer (Shimadzu UV-2550) at room temperature. FT-IR (Tensor 27, Bruker, Switzerland) spectroscopy was recorded by KBr sample holder method. The magnetization of γ-Fe_2O_3, γ-Fe_2O_3@PANI and γ-Fe_2O_3@PANI-CHB were obtained by Vibrating Sample Magnetometer (VSM, EV7, ADE, USA) at room temperature and ± 8 kOe applied magnetic field. The cyclic voltammetry characteristics of γ-Fe_2O_3@PANI and γ-Fe_2O_3@PANI-CHB were examined in the three-electrode system by CHI 660 electrochemical workstation (CHI Instruments, USA). The thermogravimetric curve of γ-Fe_2O_3, γ-Fe_2O_3@PANI, γ-Fe_2O_3@ PANI-CHB, CHB dry powders were measured by the thermal gravimetric analysis (TGA, Pyris 1 TGA, Perkin Elmer, Inc.) in the flow rate of 20 mL/min nitrogen atmosphere and heating rate of 10 °C/min. The diffraction patterns of the samples were measured by X-ray diffraction (XRD, D8 Adwance, Bruker-AXS) at the constant temperature and the diffraction angle range from 10° to 80°. The size and morphology of the product particles were measured by the transmission electron microscopy (TEM, Tecnai-12, Philip Apparatus, Inc.).

Surface modification of γ-Fe_2O_3@PANI-CHB: The surfactant poly(vinyl pyrrolidone)(PVP) was used to improve the surface properties of γ-Fe_2O_3@PANI-CHB to increase its solubility in water. The different percentages of poly(vinyl pyrrolidone) solution were prepared. Certain amounts of γ-Fe_2O_3@PANI-CHB were dissolved in the test solutions, ultrasonic vibration for 6 h and observed the suspension effect under stationary state.

RESULTS AND DISCUSSION

Characterization of γ-Fe_2O_3@PANI-CHB: The chlorambucil was dissolved in 10 mL of the acetone and it was added dropwise to 50 mL of the γ-Fe_2O_3@PANI aqueous solution for generating γ-Fe_2O_3@PANI-CHB in a homogeneous medium. While chlorambucil was dissolved in 10 mL of the chloroform and γ-Fe_2O_3@PANI-CHB in a heterogeneous medium was prepared in the same way. As the curve of γ-Fe_2O_3@PANI shown in Fig. 2a, the peaks at 1487 cm^{-1} and 1566 cm^{-1} respectively correspond to the C-C stretching vibration of the benzene ring and the quinoid ring. The peak at 1299 cm^{-1} is aromatic (C-N) stretching band of polyaniline, the broad and strong absorption peak at 1132 cm^{-1} corresponds to B-NH-B stretching vibration of polyaniline and the peak at 800 cm^{-1} is *para*-disubstituted benzene ring[36-41].

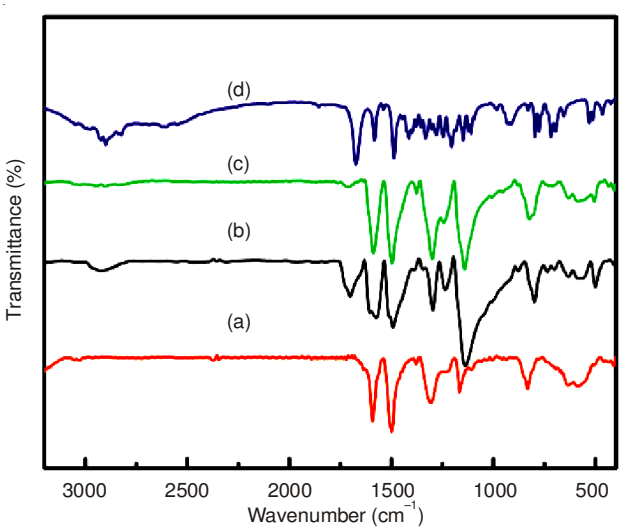

Fig. 2. FT-IR spectra of γ-Fe_2O_3@ PANI-CHB in the different synthesis conditions, (a) γ-Fe_2O_3@PANI; (b) γ-Fe_2O_3@PANI-CHB prepared in a homogeneous medium, (c) γ-Fe_2O_3@PANI-CHB prepared in a heterogeneous medium, (d) chlorambucil

A peak appears at 1701 cm^{-1} in the curve of γ-Fe_2O_3@PANI-CHB (Fig. 2b, c), which is corresponding to C=O stretching vibration peak of the chlorambucil. The C-C stretching vibration peaks of the quinoid ring and the benzene ring move to 1575 and 1492 cm^{-1}. By comparison of the two IR spectra in Fig. 2 (curve b and c), we can see that the relative intensity of the peaks at 1910 and 1701 cm^{-1} become larger and the characteristic peak at 1136 cm^{-1} that marks the polyaniline doping become the largest peak. It implied that the chlorambucil is mainly doped with quinoid structure rather

than the benzene structure and the doped level of chlorambucil in a homogeneous medium is larger than that in a heterogeneous medium. The experimental results also show that lower than 55 °C is helpful to the process of chlorambucil doped into γ-Fe_2O_3@PANI based on the effect of temperature on synthesis of γ-Fe_2O_3@PANI-CHB. This was further confirmed by UV-visible absorption that while the temperature rises to 55 °C (Fig. 3a-d), the peaks of chlorambucil at 258 and 300 nm shift to longer wavelength because of the hydrolysis of chlorambucil at higher temperature[42]. The peak at near 467 nm appears and the peak at 573 nm disappeared, which respectively came from doping peak of polyaniline by chlorambucil and caused by the quinine ring of polyaniline disappearing because of the chlorambucil doped into γ-Fe_2O_3@PANI (Fig.3e-g).

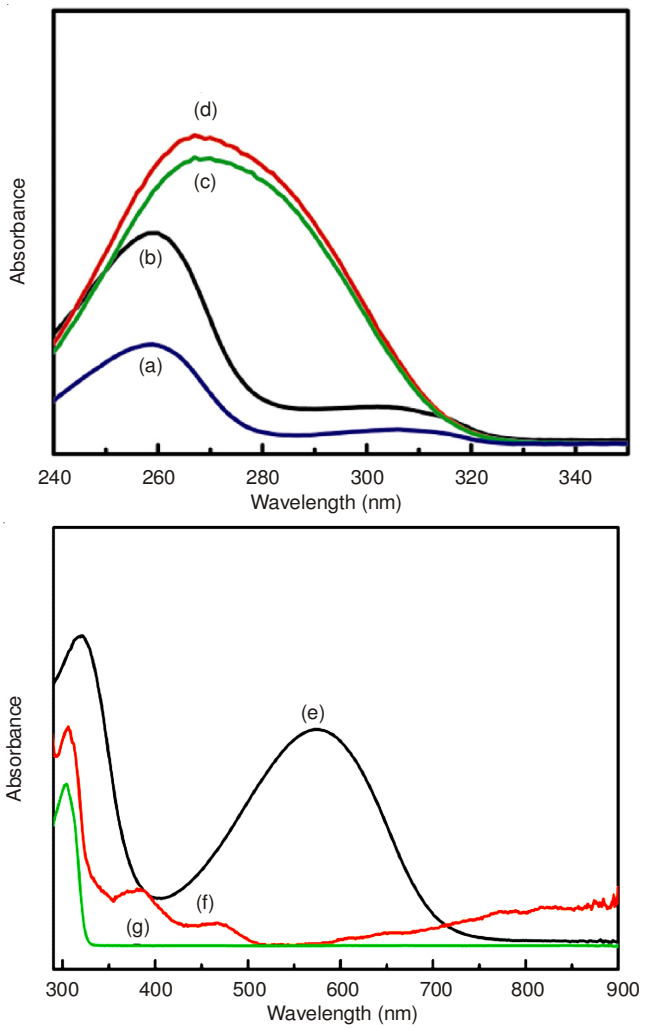

Fig. 3. UV-visible spectra of samples in the chloroform, (a) chlorambucil at 40 °C; (b) chlorambucil at 50 °C; (c) chlorambucil at 55 °C; (d) chlorambucil at 60 °C; (e) γ-Fe_2O_3@PANI; (f) γ-Fe_2O_3@PANI-CHB at 50 °C; (g) CHB at 50 °C

Fig. 4 shows the XRD patterns of chlorambucil (a), γ-Fe_2O_3 (b), γ-Fe_2O_3@PANI (c) and γ-Fe_2O_3@PANI-CHB (d). It is seen from Fig. 4a that the chlorambucil has the partial crystallization peaks in 2θ from 19° to 25°. The diffraction peaks at 2θ = 30.2°, 35.6°, 43.2°, 53.8°, 57.3° and 62.9° are corresponding to rigid structure of γ-Fe_2O_3 in Fig. 4b[43,44]. The γ-Fe_2O_3@PANI sample maintains crystal structure of γ-Fe_2O_3 after PANI wrapping γ-Fe_2O_3 and the amorphous hump peak of PANI (Fig. 4c) also appears between 18° and 23°[45,46]. After chlorambucil doped into γ-Fe_2O_3@PANI, the relative intensity of diffraction peak at 2θ = 20° that corresponds to the diffraction peaks of γ-Fe_2O_3 weaken, which is caused by the chlorambucil doped into PANI and indicate that the relative content of iron oxide decreases in the γ-Fe_2O_3@PANI-CHB (Fig. 4d).

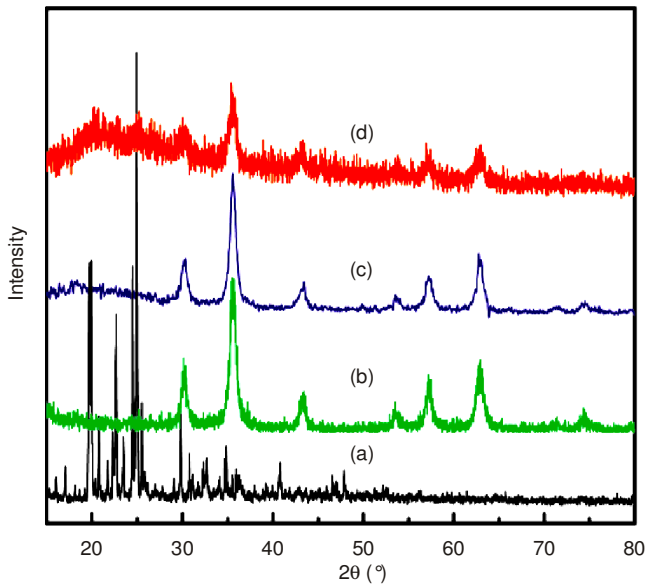

Fig. 4. XRD patterns of samples, (a) chlorambucil; (b) γ-Fe_2O_3; (c) γ-Fe_2O_3@PANI; (d) γ-Fe_2O_3@PANI-CHB

Fig.5 shows that the saturation magnetization of γ-Fe_2O_3@PANI-CHB in a homogeneous medium is 8.77 emu g^{-1}, while the γ-Fe_2O_3@PANI-CHB in a heterogeneous medium is 22.7 emu g^{-1}. According the saturation magnetization of γ-Fe_2O_3@PANI and γ-Fe_2O_3@PANI-CHB, it can be concluded that the percentage of chlorambucil in γ-Fe_2O_3@PANI-CHB is respectively 44.45 % in a homogeneous medium and 22.34 % in a heterogeneous medium. The results provide further evidence that the synthesis of γ-Fe_2O_3@PANI-CHB in a homogeneous medium has higher drug loading.

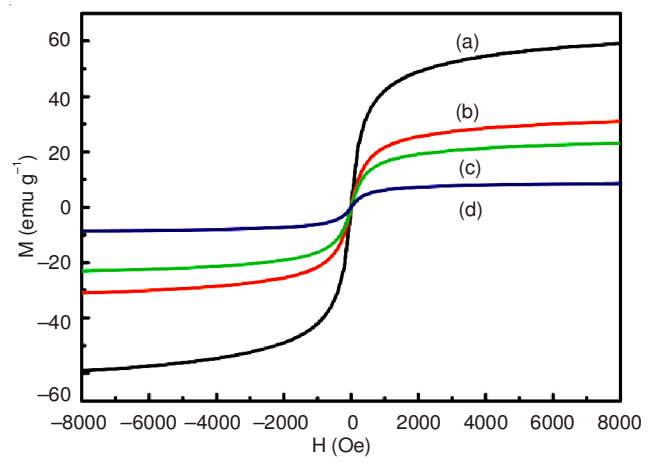

Fig. 5. Magnetization curve of different samples, (a) γ-Fe_2O_3; (b) γ-Fe_2O_3@PANI; (c) γ-Fe_2O_3@PANI-CHB prepared in a heterogeneous medium; (d) γ-Fe_2O_3@PANI-CHB prepared in a homogeneous medium

Fig. 6 is the effect of ratio of PANI/CHB on magnetization of γ-Fe_2O_3@PANI-CHB in a homogeneous medium. When the molar ratio of PANI/CHB is 1:1 to 4:1, the γ-Fe_2O_3@PANI-CHB has good superparamagnetism (Fig.6). However, the corresponding saturation magnetization of the γ-Fe_2O_3@PANI-CHB decreased with increasing proportion of the chlorambucil. When the molar ratio of PANI/CHB is 1:2, the saturation magnetization of the γ-Fe_2O_3@PANI-CHB is only 6.8 emu g^{-1}, which is too small to meet magnetic targeting requirements of the magnetic drug. The amounts of chlorambucil doped into polyaniline are lower when the proportion of PANI is too high and the efficacy of the drug is suppressed. Therefore, the molar ratio of PANI/CHB between 1:1 and 2:1 is the appropriate synthetic condition.

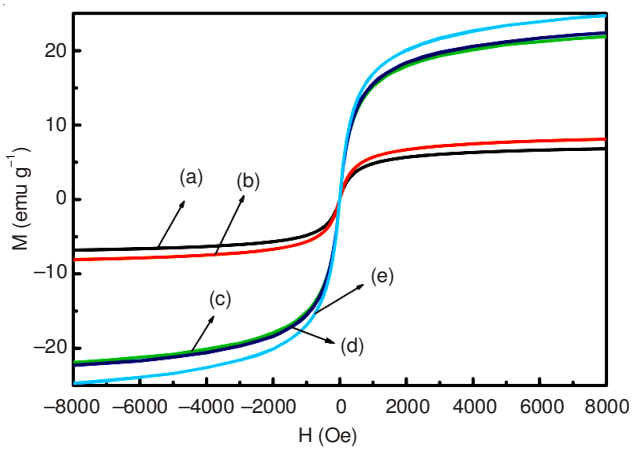

Fig. 6. Magnetization curve of γ-Fe_2O_3@PANI-CHB in different molar ratio of PANI/CHB, (a) 1:2; (b) 1:1; (c) 2:1; (d) 3:1; (e) 4:1

Fig. 7 shows the cyclic voltammetry curves of γ-Fe_2O_3@PANI-CHB at different pH values. It is seen from Fig. 7 that each curve has a pair of redox peaks in the cyclic voltammograms of γ-Fe_2O_3@PANI-CHB. When the pH value is 4, the anodic peak potential is 0.20 V and the reduction peak potential is 0.123 V. With increasing pH, the peak potential and the peak current decreased, which indicated that the redox processes of γ-Fe_2O_3@PANI-CHB were related to the concentration of H^+ (Fig.7). At pH = 7 to 8, γ-Fe_2O_3@PANI-CHB still has the electrochemical activity and the conductivity of 0.012 S cm^{-1} (four-probe technique[47]), indicating that the γ-Fe_2O_3@PANI-CHB still has good electrical conductivity after chlorambucil doped into γ-Fe_2O_3@PANI, which is benefit for the γ-Fe_2O_3@PANI-CHB to identify the diseased cells or tissues in the biological microenvironment[48].

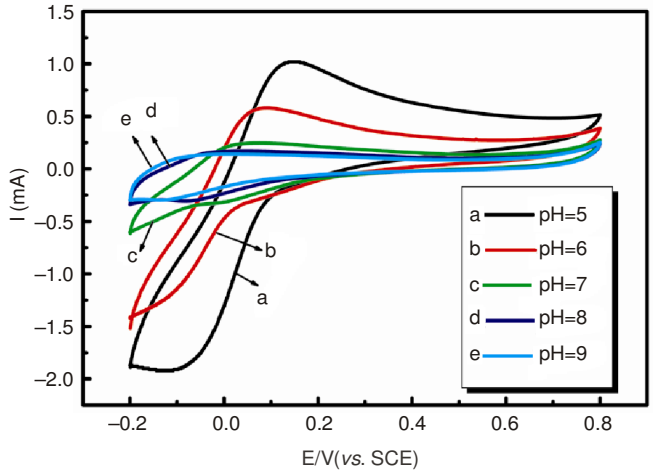

Fig. 7. Cyclic voltammetry curves of γ-Fe_2O_3@PANI-CHB at different pH values (pH = 4-8, 20 mV s^{-1})

Fig. 8 shows TG spectra of the γ-Fe_2O_3@PANI (a), γ-Fe_2O_3@PANI-CHB (b) and chlorambucil (c). It can be seen from Fig. 8a that the γ-Fe_2O_3@PANI shows four-stage weight loss: The first step (40-100 °C) corresponded to the loss of water in the polymer; the second step (about 270-359 °C) was attributed to loss of acid dopant in the polymer[49]; the third step (478-589 °C) was caused by oxidative degradation of PANI chain and the final step (651-736 °C) was due to the phase transformation from γ-Fe_2O_3 to α-Fe_2O_3[50]. The weight loss curve of γ-Fe_2O_3@PANI-CHB in Fig. 8b is somewhat similar with γ-Fe_2O_3@PANI. The γ-Fe_2O_3@PANI-CHB also shows four-stage weight loss: The first step (40-100 °C) was the loss of water in the sample; the second step (about 206-308 °C) was due to the decomposition of chlorambucil and loss of acid dopant in the polymer; the third step (310-470 °C) was attributed to degradation of PANI chain; and the final step (525-736 °C) was due to the phase transformation from γ-Fe_2O_3 to α-Fe_2O_3. In Fig. 8c, the weight loss curve of chlorambucil indicated that the decomposition temperature of chlorambucil was about 300-350 °C. Compared Fig. 8b with Fig. 8a and Fig. 8c, chlorambucil has been doped into γ-Fe_2O_3@PANI.

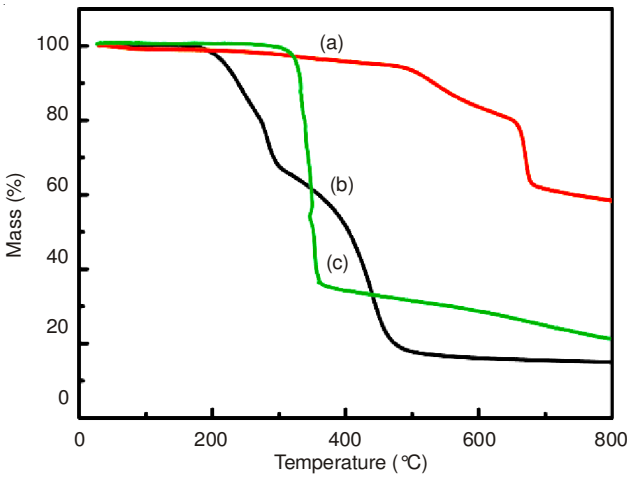

Fig. 8. Thermoanalysis of samples, (a) γ-Fe_2O_3@PANI, (b) γ-Fe_2O_3@PANI-CHB, (c) CHB

The γ-Fe_2O_3@PANI and γ-Fe_2O_3@PANI-CHB particles partially aggregate, but the surface morphology is relatively clear and easy to identify (Fig. 9). Both of γ-Fe_2O_3@PANI and γ-Fe_2O_3@PANI-CHB are spherical granules and particle diameter of the latter (< 20 nm) is larger than that of the former (< 10 nm), which further confirms that chlorambucil is successfully doped into γ-Fe_2O_3@PANI. The γ-Fe_2O_3@PANI-CHB meets characteristics of superparamagnetic and biocompatible and nano-size (< 100 nm) for a magnetic targeting drug.

Suspensibility of the γ-Fe_2O_3@PANI-CHB[51,52]: Fig. 10 shows the changes of the suspensibility of γ-Fe_2O_3@PANI-CHB with time in 4, 8, 10, 16, 20, 22 and 28 % weight percentage of poly(vinyl pyrrolidone) aqueous solutions.

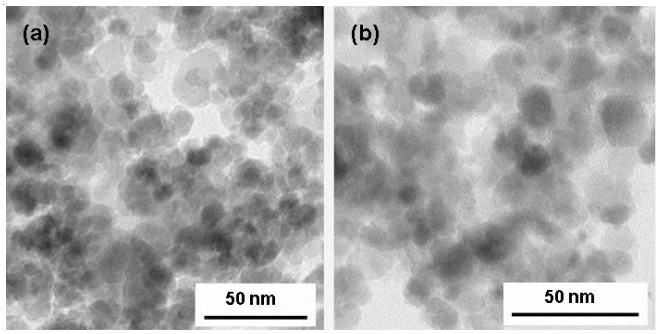

Fig. 9. TEM images of samples, (a) γ-Fe_2O_3@PANI; (b) γ-Fe_2O_3@PANI-CHB

The delamination of γ-Fe_2O_3@PANI-CHB solution occurred in 4, 8 and 28 % of poly(vinyl pyrrolidone) aqueous solutions after one week and 10 % of poly(vinyl pyrrolidone) solution was delamination after one month, while the γ-Fe_2O_3@PANI-CHB nanoparticles had good suspensibility in 16, 20 and 22 % of poly(vinyl pyrrolidone) aqueous solutions after two months. It can be seen that the γ-Fe_2O_3@PANI-CHB in 16, 20 and 22 % of poly(vinyl pyrrolidone) aqueous solutions can be used as magnetic targeting drug.

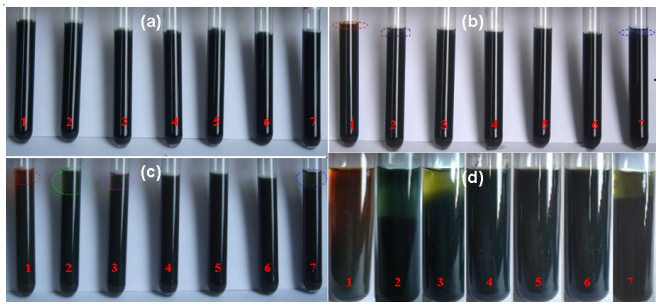

Fig. 10. Solubilization effect changes with time in the non-ionic surfactant poly(vinyl pyrrolidone) solution, (a) one day; (b) one week; (c) one month; (d) two months.

***in vitro* studies regulated by external magnetic field for γ-Fe_2O_3@PANI-CHB**: To demonstrate the effect of an external magnetic field on regulation, the γ-Fe_2O_3@PANI-CHB solution was studied in the presence of a magnetic field by using a 3 mm silicone tube to mimic a blood vessel[53]. A certain concentration of γ-Fe_2O_3@PANI-CHB was injected into the reservoir bottle and connected the mimic device in the Fig. 11. The test tube 1 was used to collect the original drug solution (open piston 1, 2, close the piston 3; here piston 1 can also be used to adjust the flow rate). Tube 2 was used to obtain the drug solution that flows through the magnetic field (open piston 1, 3, 4, close the piston 2, 5). The test tube 3 was used to collect the drug solution, which was gathered at the site of 3000 Guass magnetic field (open piston 1, 3, 5, 6, turn off the piston 2, 4). The certain amount of γ-Fe_2O_3@PANI-CHB was dissolved in 16 % poly(vinyl pyrrolidone) aqueous solution by ultrasound for 6 h and to conduct *in vitro* magnetization studies of γ-Fe_2O_3@PANI-CHB. Results were shown in Table-1.

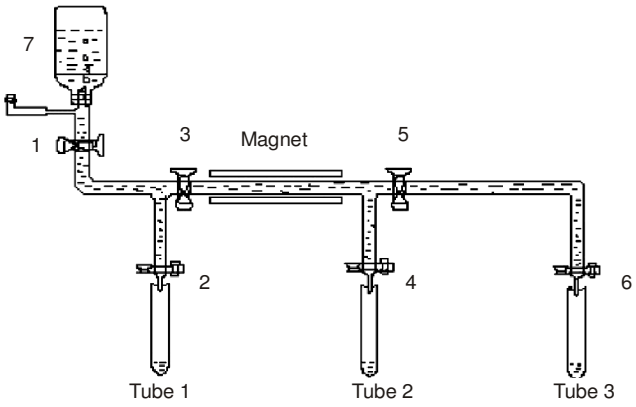

Fig. 11. Schematic diagram of γ-Fe_2O_3@PANI-CHB simulation in a mimic blood vessel by the application of magnetic field (1, 2, 3, 4, 5 and 6 parts of the figure are the control piston; the 7 part is reservoir bottle)

At different flow rates, the solutions that flowed within 8 min were collected. When the flow rate was 0.0187 g s^{-1}, the aggregation concentration of γ-Fe_2O_3@PANI-CHB was 2 times higher than the original concentration in the 3000 Gauss magnetic field and the concentration of the drug in other parts reduced effectively to 1/3 of the original drug concentration after flowing over the magnetic field (Table-1). When the flow rate was 0.1118 g s^{-1}, the aggregation concentration of γ-Fe_2O_3@PANI-CHB was 6 times higher than the original concentration in the 3000 Gauss magnetic field, while the concentration of the drug in other parts reduced effectively to 1/2 of the original drug concentration after flowing over the magnetic field. It obviously shows that γ-Fe_2O_3@PANI-CHB can be regulated by an external magnetic field.

Toxicity of γ-Fe_2O_3@PANI and γ-Fe_2O_3@PANI-CHB on cells: MDCK[54] cells were chosen to explore the pharmacological toxicity of γ-Fe_2O_3@PANI and γ-Fe_2O_3@PANI-CHB. If the γ-Fe_2O_3@PANI-CHB did not have role of the killing MDCK cells, the MDCK cell culture solution showed yellow-brown after the cells producing metabolites. Once the γ-Fe_2O_3@PANI-CHB could kill the MDCK cells, the MDCK cells were inhibited or death and no longer produced metabolites and the MDCK cell culture medium maintained the original red-brown.

5, 20 and 100 µL of the @PANI solution were added to each beaker. The beakers from left to right presented pale yellow, bright yellow and dark yellow in turn (Fig. 12a), which

TABLE-1
GATHERED CONCENTRATION OF γ-FE_2O_3@PANI-CHB UNDER THE CONDITIONS OF THE MAGNETIC AND NON-MAGNETIC FIELD AT DIFFERENT FLOW RATES

Entry	Flow rate (g s^{-1})	C_1 (mg mL^{-1})	C_2 (mg mL^{-1})	C_3(mg $mL^{-1)}$
1	0.0187	2.4	0.8125	4.8
2	0.1118	2.4	1.2428	14.4

C_1 (the concentration of γ-Fe_2O_3@PANI-CHB in the original solution), C_2 (the concentration of γ -Fe_2O_3@PANI-CHB after the solutions flowing through the magnetic field), C_3 (the concentration of γ -Fe_2O_3@PANI-CHB stranded in the parts of the magnetic field)

indicated that γ-Fe_2O_3@PANI had no toxic side effects on MDCK cells and the γ-Fe_2O_3@PANI has bio-security features. Then 5, 20 and 100 μL of the γ-Fe_2O_3@PANI-CHB solution were added to every beaker. When the addition amount was 5 μL, the cell culture medium was yellow and the cells continued to grow and produce yellow metabolites, which indicated that the γ-Fe_2O_3@PANI-CHB has no killing effect on the cells in the concentration. When the addition amount was 20 μL, the cell culture medium presented red-brown, which indicated that the γ-Fe_2O_3@PANI-CHB had partially killing effect or weakly killing effect on the MDCK cells in the concentration. While 100 μL of γ-Fe_2O_3@PANI-CHB was added, the cell culture medium was dark red, which indicated that the γ-Fe_2O_3@PANI-CHB is a strong lethal for the MDCK cells in the concentration and results in the MDCK cell death in a short time and the MDCK cell culture medium showed approximate cytosol colours (Fig. 12b). In conclusion, the γ-Fe_2O_3@PANI has bio-security and no toxic side effects on MDCK cells and γ-Fe_2O_3@PANI-CHB has a killing effect on the MDCK cells.

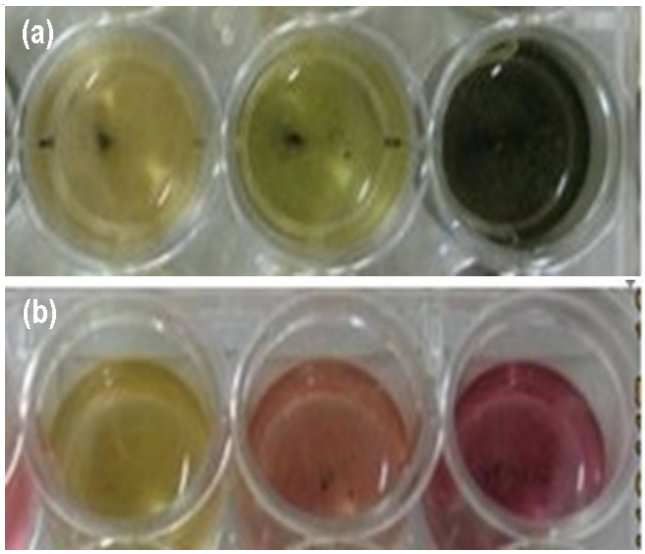

Fig. 12. Killing effect on cells in the different concentrations of γ-Fe_2O_3@PANI (a) and γ-Fe_2O_3@PANI-CHB (b)

Conclusion

The γ-Fe_2O_3@PANI-CHB as a new kind of composite has been synthesized. The chlorambucil was fixed in the γ-Fe_2O_3@PANI based on the unique doping-dedoping mechanism of the polyaniline, which don't change doped groups of the original chlorambucil. The newly synthesized composite γ-Fe_2O_3@PANI-CHB highlights the unique superparamagnetic and electrochemical activity. Non-ionic surfactant poly(vinyl pyrrolidone) plays a good stabilization effect on the γ-Fe_2O_3@PANI-CHB and the particle size of γ-Fe_2O_3@PANI-CHB in the suspended state still meets the requirements of magnetic targeting (< 100 nm). The γ-Fe_2O_3@PANI has bio-security and no toxic side effects on MDCK cells and γ-Fe_2O_3@PANI-CHB has a killing effect on the MDCK cells. The study provides an academic foundation for developing some new drugs of anticancer.

ACKNOWLEDGEMENTS

This project was supported by National Science Foundation of China (No. 20873119) and by the Priority Academic Program Development of Jiangsu Higher Education Institutions. Part of data was from Testing Center of Yangzhou University.

REFERENCES

1. A.G. Macdiarmid, J.-C. Chiang, M. Halpern, W.-S. Huang, S.-L. Mu, L.D. Nanaxakkara, S.W. Wu and S.I. Yaniger, *Mol. Cryst. Liq. Cryst.*, **121**, 173 (1985).
2. H. Zengin, W. Zhou, J. Jin, R. Czerw, D.W. Smith, L. Echegoyen, D.L. Carroll, S.H. Foulger and J. Ballato, *Adv. Mater*., **14**, 1480 (2002).
3. M.M. Ayad and E.A. Zaki, *Eur. Polym. J*., **44**, 3741 (2008).
4. S. Li, L. Tang, R. Tang and J. Kan, *Asian J. Chem*, **22**, 415 (2010).
5. S. Sinha, S. Bhadra and D. Khastgir, *J. Appl. Polym. Sci*., **112**, 3135 (2009).
6. Z. Ma, Q. Shen and J. Kan, *Asian J. Chem*., **25**, 8574 (2013).
7. S. Bhadra, D. Khastgir, N. Singha and J.H. Lee, *Prog. Polym. Sci*., **34**, 783 (2009).
8. S.A. Ghani and H.C. Young, *J. Physiol. Sci*., **21**, 81 (2010).
9. A. Rahy, J. Bae, A.M. Wu, S.K. Manohar and D.J. Yang, *Polym. Adv. Technol*., **22**, 664 (2011).
10. F.Z. Silveira, G.W. Duarte, C.G. Tachinski, R. Piletti, J. Fiori Jr., M. Peterson, H.G. Riella and M.A. Fiori, *J. Appl. Polym. Sci*., **128**, 430 (2013).
11. P. Saini, V. Choudhary, K.N. Sood and S.K. Dhawan, *J. Appl. Polym. Sci*., **113**, 3146 (2009).
12. A.S. Roy, K.R. Anilkumar and M.V.N.A. Prasad, *J. Appl. Polym. Sci*., **123**, 1928 (2012).
13. M.O. Ansari and F. Mohammad, *J. Appl. Polym. Sci*., **124**, 4433 (2012).
14. E.N. Konyushenko, N.E. Kazantseva, J. Stejskal, M. Trchova, J. Kovarova, I. Sapurina, M.M. Tomishko, O.V. Demicheva and J. Prokes, *J. Magn. Magn. Mater*., **320**, 231 (2008).
15. V. Babayan, N.E. Kazantseva, I. Sapurina, R. Moucka, J. Stejskal and P. Saha, *J. Magn. Magn. Mater*., **333**, 30 (2013).
16. J. Hongxia, L. Qiaoling, Y. Yun, G. Zhiwu and Y. Xiaofeng, *J. Magn. Magn. Mater*., **332**, 10 (2013).
17. C.H. Wang, Y.Q. Dong, K. Sengothi, K.L. Tan and E.T. Kang, *Synth. Met*., **102**, 1313 (1999).
18. X. Yan, J. Chen, J. Yang, Q. Xue and P. Miele, *ACS Appl. Mater. Interfaces*, **2**, 2521 (2010).
19. M.Y. Li, Y. Guo, Y. Wei, A.G. MacDiarmid and P.I. Lelkes, *Biomaterials*, **27**, 2705 (2006).
20. S. Ben-Valid, H. Dumortier, M. Décossas, R. Sfez, M. Meneghetti, A. Bianco and S. Yitzchaik, *J. Mater. Chem*., **20**, 2408 (2010).
21. P.R. Bidez, S. Li, A.G. MacDiarmid, E.C. Venancio, Y. Wei and P.I. Lelkes, *J. Biomater. Sci. Polym. Ed*., **17**, 199 (2006).
22. A.K. Gupta and M. Gupta, *Biomaterials*, **26**, 3995 (2005).
23. T. Neuberger, B. Schöpf, H. Hofmann, M. Hofmann and B. von Rechenberg, *J. Magn. Magn. Mater*., **293**, 483 (2005).
24. H. Ehrsson, S. Eksborg, I. Wallin and S. Nilsson, *J. Pharm. Sci*., **69**, 1091 (1980).
25. A.G. Bosanquet and H.E. Clarke, *Cancer Chemother. Pharmacol*., **18**, 176 (1986).
26. M. Suwalsky, P. Hernández, F. Villena and C.P. Sotomayo, *Z. Naturforsch. C*, **54**, 1089 (1999).
27. L.J. Parker, S. Ciccone, L.C. Italiano, A. Primavera, A.J. Oakley, C. Morton, N.C. Hancock, M.L. Bello and M.W. Parker, *J. Mol. Biol*., **380**, 131 (2008).
28. H. Skribek, R. Otvos, E. Flaberg, N. Nagy, L. Markasz, S. Eksborg, T. Masszi, A. Kozma, E. Adam and A. Miseta, *Exp. Hematol*., **38**, 1219 (2010).
29. R.D. Goff and J.S. Thorson, *J. Med. Chem*., **53**, 8129 (2010).
30. R.B. Kaner, *Synth. Met*., **125**, 65 (2001).
31. A. Baba, R.C. Advincula and W. Knoll, *J. Phys. Chem. B*, **106**, 1581 (2002). (Affiliation Information).
32. J.D. Holbrey, W.M. Reichert, R.P. Swatloski, G.A. Broker, W.R. Pitner, K.R. Seddon and R.D. Rogers, *Green Chem*., **4**, 407 (2002).
33. A. Navalón, R. Blanc, L. Reyes, N. Navas and J.L. Vílchez, *Anal. Chim. Acta*, **454**, 83 (2002).

34. B.Z. Tang, Y.H. Geng, J.W.Y. Lam, B.S. Li, X. Jing, X. Wang, F. Wang, A.B. Pakhomov and X.X. Zhang, *Chem. Mater*., **11**, 1581 (1999).
35. Y.S. Kang, S. Risbud, J.F. Rabolt and P. Stroeve, *Chem. Mater*., **8**, 2209 (1996).
36. S.L. Mu and J.Q. Kan, *Synth. Met*., **98**, 51 (1998).
37. D.W. Hatchett, M. Josowicz and J. Janata, *J. Phys. Chem. B*, **103**, 10992 (1999).
38. P.D. Gaikwad, D.J. Shirale, V.K. Gade, P.A. Savale, K.P. Kakde, H.J. Kharat and M.D. Shirsat, *Bull. Mater. Sci*., **29**, 417 (2006).
39. Y. Cao, P. Smith and C. Yang, *Synth. Met*., **69**, 191 (1995).
40. J.K. Avlyanov, Y.G. Min, A.G. MacDiarmid and A.J. Epstein, *Synth. Met*., **72**, 65 (1995).
41. Y.G. Min, Y.N. Xia, A.G. MacDiarmid and A.J. Epstein, *Synth. Met*., **69**, 159 (1995).
42. H. Ehrsson, S. Eksborg, I. Wallin and S.-O. Nilsson, *J. Pharm. Sci*., **89**, 1091 (1980).
43. H.Y. Zhu, R. Jiang, L. Xiao and G.M. Zeng, *Bioresour. Technol*., **101**, 5063 (2010).
44. K.R. Reddy, W. Park, B.C. Sin, J. Noh and Y. Lee, *J. Colloid Interface Sci*., **335**, 34 (2009).
45. Y.Y. Wang, X.L. Jing and J.H. Kong, *Synth. Met*., **157**, 269 (2007).
46. J.F. Chen, Y.T. Xu, Y.F. Zheng, L.Z. Dai and H.H. Wu, *C. R. Chim*., **11**, 84 (2008).
47. R.K. Hiremath, M.K. Rabinal and B.G. Mulimani, *Rev. Sci. Instrum*., **77**, 126106 (2006).
48. J.K. Nicholson, J. Connelly, J.C. Lindon and E. Holmes, *Nat. Rev. Drug Discov*., **1**, 153 (2002).
49. X.H. Wang, Y.H. Geng, L.X. Wang, X.B. Jing and F.S. Wang, *Synth. Met*., **69**, 265 (1995).
50. C.W. Lee, S.S. Jung and J.S. Lee, *Mater. Lett*., **62**, 561 (2008).
51. M.J. Rosen, F. Li, S.W. Morrall and D.J. Versteeg, *Environ. Sci. Technol*., **35**, 954 (2001).
52. W.J.W. Pape, U. Pfannenbecker, H. Argembeaux, M. Bracher, D.J. Esdaile, S. Hagino, Y. Kasai and R.W. Lewis, *Toxicol. in Vitro*, **13**, 343 (1999).
53. G.A. Flores and J. Liu, *Eur. Cell. Mater*., **3 (Suppl. 2)**, 9 (2002).
54. F. Lang and M. Paulmichl, *Kidney Int*., **48**, 1200 (1995).